CONF-900542--8
RECEIVED BY OSTI
MAY 29 1990

THE EFFECTS OF DIFFERENT DIFFUSION SOURCES ON SILICON SOLAR CELL RECOMBINATION PROPERTIES

SAND--89-2488C

DE90 011235

Douglas S. Ruby and John D. McBrayer

Sandia National Laboratories
Albuquerque, New Mexico 87185

ABSTRACT

The importance of forming low-recombination passivated emitter regions while maintaining high bulk recombination lifetimes has been clearly established as necessary for the fabrication of high-efficiency silicon solar cells. Many different types of diffusion sources are available for performing the emitter diffusions for each dopant species. Each could affect device quality in a unique way, and each has particular attributes that determine its cost-effectiveness.

In this study, we compared the effects of PH_3 and $POCl_3$ diffusion sources on recombination lifetimes and emitter saturation currents. We also examined the relative costs associated with each, including material, capital and safety costs. We found that while both sources can produce equivalent high-performance cells, PH_3 may have a higher yield in this regard. Because the safety concerns regarding PH_3 can be addressed in a cost-effective manner, it has a cost advantage over $POCl_3$ when used for mass production.

INTRODUCTION

The most efficient silicon solar cells fabricated to date all have several features in common. First, they are highly effective at coupling light into the cell. Once inside, the light generates close to the maximum possible number of electron-hole pairs. These are then almost all collected and delivered to the cell terminals at the highest possible voltage. The last parameter, cell voltage, is the area most in need of improvement and the focus of several recent research activities. Recent successes at obtaining high cell voltages have been the result of reductions in the recombination rate of excess carriers at high carrier concentrations. This follows from the ideal-diode relationship:

$$V_{oc} = (kT/q) \cdot \ln(J_{sc}/J_o) \qquad (1)$$

where V_{oc} = open-circuit voltage,
J_{sc} = short-circuit current density,
J_o = saturation current density, and
kT/q = thermal voltage.

This work was supported by the U.S. Department of Energy under contract DE-AC04-76DP00789.

MASTER

DISTRIBUTION OF THIS DOCUMENT IS UNLIMITED

HANWHA v. MAXEON
IPR2024-01203
HANWHA 1086

DISCLAIMER

This report was prepared as an account of work sponsored by an agency of the United States Government. Neither the United States Government nor any agency thereof, nor any of their employees, makes any warranty, express or implied, or assumes any legal liability or responsibility for the accuracy, completeness, or usefulness of any information, apparatus, product, or process disclosed, or represents that its use would not infringe privately owned rights. Reference herein to any specific commercial product, process, or service by trade name, trademark, manufacturer, or otherwise does not necessarily constitute or imply its endorsement, recommendation, or favoring by the United States Government or any agency thereof. The views and opinions of authors expressed herein do not necessarily state or reflect those of the United States Government or any agency thereof.

DISCLAIMER

Portions of this document may be illegible in electronic image products. Images are produced from the best available original document.

By reducing excess-carrier recombination, the saturation current J_o can be lowered and the cell voltage can be increased.

Recombination can occur in one of several possible ways. Carriers can recombine in the lightly doped bulk region of the cell, the more heavily doped emitter regions, or at the cell surfaces. Bulk recombination is minimized by using high-lifetime starting material and clean, careful processing techniques which maintain this lifetime (1,2). Cells can be made thin enough that the carrier diffusion length greatly exceeds the distance to the collecting junction. Thin cells also have reduced levels of Auger recombination, which increases with cell volume.

Recombination at cell surfaces is minimized by the growth of a thermal, passivating oxide over all regions that are not directly contacted by metal. Extremely low surface recombination velocities have been obtained by several groups using methods that include careful pre-cleaning, chlorine gettering, controlled heating and cooling rates, and hydrogen annealing (3,4). Special precautions are necessary to prevent damage to passivating surfaces by exposure to long-term or concentrated UV radiation (5). Other methods used to reduce the surface recombination rate include the use of minority carrier reflectors, which are doping gradients that form fields to repel minority carriers from high-recombination velocity surfaces (6). These methods can make bulk and surface recombination negligible compared to that in the emitters, so that the saturation current density is dominated by the emitter component J_{oe}.

For many high-performance silicon cells, recombination in the heavily-doped diffused regions remains as the performance-limiting component of recombination at intermediate concentration levels (7). Several approaches have been studied in an attempt to reduce this diffused region (emitter) contribution to recombination. In the point-contact cell design, emitter areas are restricted to a few percent of total cell area, so that their contribution to recombination is reduced (7).

In the passivated emitter solar cell (PESC, PERC, PERL) designs, the emitter regions are passivated by a high-quality oxide over most of the cell area, and only a small fraction is contacted by high-recombination metal regions (4,8). Under the metal, a heavily-doped deep diffusion is used to reduce recombination at the metal/silicon interface.

Alternative contact materials have also been used to try to form low-recombination contact regions. These include the use of doped-polycrystalline Si to form contacts to n- and p-type emitter regions (9,10). Semi-insulating polycrystalline Si (SIPOS) has also been studied as a possible contact material (11).

Although various doping sources have been used by different research groups, no systematic study has been done to determine which source is superior in terms of maintaining high bulk recombination lifetime and forming low-J_{oe} emitter regions. Many different types of diffusion sources are available for performing the emitter diffusions for each dopant species. One group has had good results using doped CVD-oxides for both n- and p-type dopant sources (12). They have fully characterized the dependence of J_{oe} on surface phosphorus concentration and junction depth for this doping source (13). Other groups have succeeded in producing 25% efficient solar cells using $POCl_3$ or solid P_2O_5 wafers, while industry commonly employs PH_3 because of its suitability for mass production.

This paper describes the results of a comparison between the use of PH_3 and $POCl_3$ to form low-recombination emitters for silicon solar cells. The two dopant sources used in this study were compared experimentally on the basis of their effect on J_{oe} and bulk photogenerated-carrier recombination lifetime τ_b.

EXPERIMENTAL TECHNIQUES

In this study, high-resistivity, n-type, (100)-oriented float zone (FZ) and magnetic Czochralski (MCZ) silicon wafers were used. Bulk resistivities in excess of 300 Ω-cm were used so that the base would be in high-level injection during lifetime measurements, while the emitter remained in low-level injection. This allowed the emitter and base components of recombination to be separated (12). Microwave photoconductance decay (PCD) was used to measure the emitter and bulk recombination in these wafers, and more detailed information regarding this technique is provided elsewhere (14).

The wafers were received lapped and unpolished. They were initially prepared by etching about 23 μm from each side in NaOH or KOH solution to remove residual saw and lapping damage. Then, all wafers were simultaneously cleaned using the same procedure, which consisted of a short buffered oxide etch, followed by a 10-minute soak in 40°C Summa cleaning solution, and a 6-minute isotropic etch in 50:1 HNO_3:HF solution. The wafers then received a short 30-second dip in

50:1 H_2O:HF solution before being rinsed, dried, and loaded into the diffusion furnace.

The diffusions were done in a quartz-tube furnace using either $POCl_3$ or PH_3 as the dopant source. In the case of $POCl_3$ diffusions, the wafers were pushed at 800°C and ramped up to 825°C at 5°C/min in an atmosphere of 90% N_2 and 10% O_2. After 10 minutes of temperature stabilization, the atmosphere was changed to about 82% O_2 and 17% N_2 while flowing 200 mg/min of $POCl_3$ for 20 minutes. The wafers were then allowed to soak in N_2 at this temperature for another 25 minutes to allow them to absorb more phosphorus before the temperature was ramped down at 5°C/min in N_2/O_2 to 800°C, when they were unloaded.

In the case of PH_3 diffusions, the wafers were pushed, pulled, and allowed to stabilize at 800°C in 90% N_2/10% O_2. The phosphorus deposition took place for 2 minutes at 800°C in an atmosphere of 91% N_2, 6% O_2, and 2.5% of a mixture of 15% PH_3 in N_2. The wafers were soaked in N_2 for 10 minutes before unloading.

Sheet resistance values obtained using 4-point probe measurements for PH_3 wafers were typically around 275 Ω/□ after the predeposition diffusion, while those for $POCl_3$ wafers were around 130 Ω/□. At this point, the phosphosilicate glass (PSG) was stripped from all the wafers in buffered oxide etch. It was found that the final sheet resistance of the emitters was very sensitive to the duration of this etch, presumably due to removal of different amounts of phosphorus which has been shown to pile up at the PSG/Si interface during PSG growth (15,16).

At this point, undiffused control wafers were added to the lot, and all received a 30 second dip in 50:1 H_2O:HF before being rinsed, dried and loaded into the furnace for a dry oxidation/drive-in diffusion. The wafers were loaded in 90% Ar/ 10% O_2, and the temperature was ramped at 5°C/min to 950°C. The temperature stabilized for 15 minutes before an atmosphere of pure O_2 was introduced for one hour. A post-oxidation anneal in Ar for 15 minutes ensued before ramping the temperature down and unloading at 800°C. Finally, the wafers received a forming gas anneal at 450°C in 12% H_2/ 78% Ar for 20 minutes.

These diffusions result in emitter sheet resistances in the range of 40-100 Ω/□. This is the range that has been found to optimize solar cell efficiency for bifacially-contacted, single-front-diffusion cells (17). Typical doping profiles obtained by SIMS measurements for each diffusion source are shown in Fig. 1. Care was taken to generate profiles with similar surface concentrations, since J_{oe} has been shown to be a sensitive function of this parameter (13,18).

After processing, J_{oe} and τ_b were measured using the microwave PCD technique. These measurements were made both with the passivating oxide in place, and then again with it removed. This allowed both passivated and unpassivated emitter saturation currents to be measured, and

TYPICAL EMITTER DOPANT PROFILES

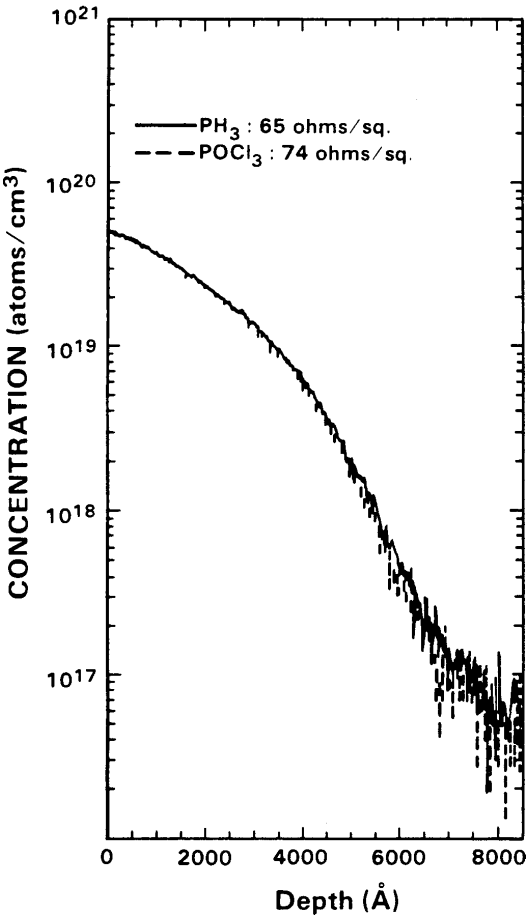


Figure 1. Doping profiles obtained by SIMS measurements for two wafers after the drive-in diffusions. The surface concentration and depth-dependence for the two doping sources are very similar.

provided a check of the experimental method, since the measured bulk lifetime value remained essentially unchanged.

RESULTS

The dependence of J_{oe} on emitter sheet resistance R_s for both doping sources is shown in Fig. 2. The values for oxide-passivated emitters show a general decrease in J_{oe} for increasing values of R_s. Both the values and the trend are in good agreement with the results of earlier studies (12,13). Using a PC-1D analysis, these values of J_{oe} for this range of sheet resistances indicate a passivated-surface recombination velocity of about 8×10^3 cm/s (19).

It is evident that both $POCl_3$ and PH_3 can produce equivalently low J_{oe} values for similar values of R_s. However, it is also clear that a significant fraction of the wafers doped with $POCl_3$ exhibit J_{oe} values that are higher than the others by more than the 95% confidence limits of

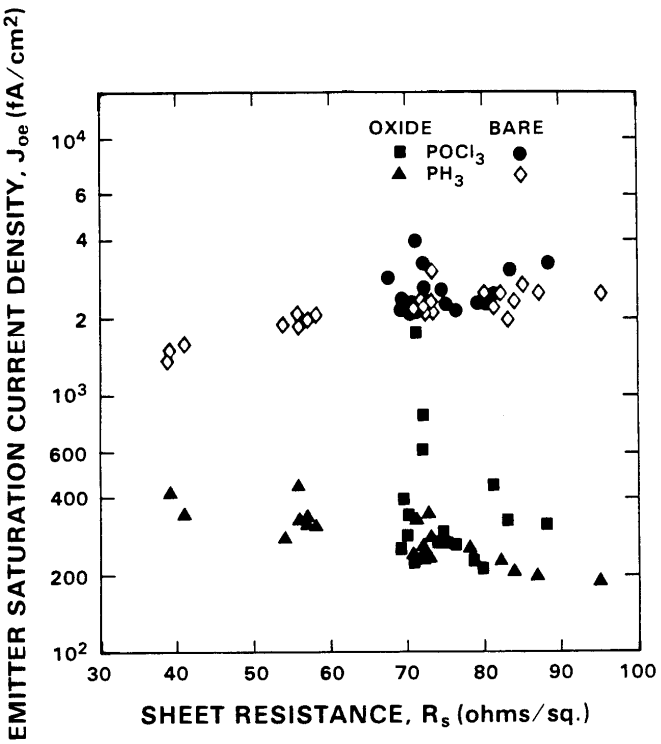


Figure 2. Dependence of J_{oe} on R_s for both doping sources for oxide-passivated and bare wafers. The uncertainty in the measurement is ±10%.

the measurement (±10%).

After the wafers were stripped bare of oxide, the J_{oe} values exhibited an increasing trend with increasing values of R_s. These values are also in general agreement with earlier work, which gives values of J_{oe} for unpassivated emitters covered with Al (12). A PC-1D analysis in this case indicates an unpassivated surface recombination velocity of about 2×10^6 cm/s.

Most of the J_{oe} values for the bare diffused wafers lie within a fairly narrow band for both dopant types with the exception of several $POCl_3$-doped wafers. These anomalous wafers exhibit higher recombination rates than can be accounted for even with a surface recombination velocity of 1×10^7 cm/s, the thermal velocity for carriers in Si. This is an indication that an abnormally large amount of recombination in the bulk of the emitters is taking place.

A plot of the dark PCD lifetime τ, which is measured in the absence of steady background illumination, is shown in Fig. 3 for several of the diffusion lots studied in this work . The dark PCD lifetime τ was used instead of τ_b extracted from the J_{oe} measurement because it could be measured more precisely. τ is determined primarily by recombination in the bulk, but does include a small component due to recombination in the emitters and at the surface. Therefore, τ represents a lower bound on the bulk recombination lifetime τ_b. It is clear that most of the diffusions resulted in bulk lifetimes more than

adequate for high-efficiency solar cells. It should be remembered that $\tau_b > 0.3$ ms results in an ambipolar diffusion length $L_D > 700$ μm, which is several times the optimum thickness of a high-efficiency Si cell with light-trapping.

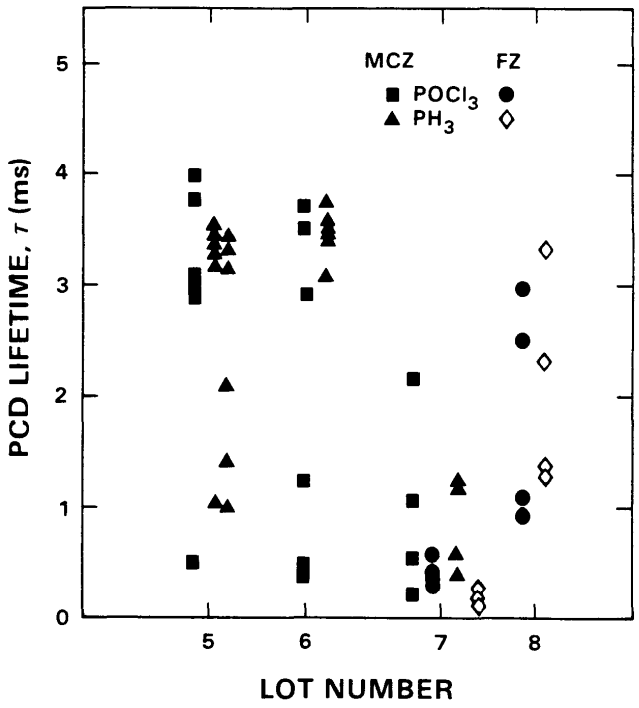


Figure 3. PCD lifetime of wafers after diffusion for several lots for both doping sources and two wafer material types (MCZ and FZ). The accuracy of the measurement is ±5%.

No clear distinction can be made between the doping sources regarding their effect on τ_b. Both can produce high lifetimes in MCZ as well as FZ wafers. When ultra-high (>1 ms) lifetimes were not obtained, as was the case for lot 7, the two doping sources also appear equivalent; i.e., one does not getter bulk impurities better than the other.

DISCUSSION

The wafers in this study consisted of randomly selected high-lifetime starting material and were all processed simultaneously and in an identical manner except for the phosphorus diffusion source. Yet, for wafers with similar doping profiles, a significant fraction of those doped using $POCl_3$ exhibited anomalously high J_{oe} values, indicative of excessive recombination in the emitters. The chemical reactions taking place during the diffusions are

$$4\ POCl_3 + 3\ O_2 \Rightarrow 2\ P_2O_5 + 6\ Cl_2 \quad (8)$$

$$2\ PH_3 + 4\ O_2 \Rightarrow P_2O_5 + 3\ H_2O \quad (9)$$

and

$$2\ P_2O_5 + 5\ Si \Rightarrow (5\ SiO_2 + 4\ P) = PSG \quad (10)$$

The primary chemical difference between using the two doping sources is that Cl_2 is present when $POCl_3$ is used and H_2O is present when PH_3 is used. Chlorine is known to getter metallic impurities and crystal imperfections during oxide growth, but is also associated with etching of the silicon surface when used inappropriately (23). We can speculate that because of its highly reactive nature, Cl_2 may sometimes induce surface defects to form, which then increase emitter recombination when using $POCl_3$. On the other hand, the PH_3 diffusion process appears to be more fault-tolerant.

COST ANALYSIS

A cost comparison of the two diffusion sources has been made based on costs incurred during construction and start-up of Sandia's Photovoltaic Device Fabrication Laboratory (PDFL) during the years 1987-1989. We started with a comparison of the costs of dopant source materials utilized during a diffusion. It was found that the deposition of 350 Å of PSG by each source was adequate for the emitter R_s values sought here. The relative cost of dopant material consumed is shown in Table 1. The result is that the cost of $POCl_3$ used is about 47 times that of PH_3 for an equivalent emitter diffusion.

TABLE 1
Cost of dopant source used to form 350 Å of PSG on a lot containing 25 wafers.

	Quantity (moles)	Cost/Mole ($/M)	Cost/Lot ($)
PH_3	3.3×10^{-3}	30	0.10
$POCl_3$	2.6×10^{-2}	180	4.70

The cost of materials consumed is only part of the total cost which must be considered. The capital cost associated with the use of each source also must be included. In the case of PH_3, because of its highly toxic nature, many safety precautions need to be taken that add to the cost of its use.

Probably the single most important safety precaution that can be taken when using any cylinder of compressed toxic gas costs nothing at all. Specialty gas vendors will supply cylinders with a Flow Restricting Orifice (FRO) installed at little or no additional cost. An FRO is a threaded plug with a small (typically 0.006 inch) hole through it which is screwed inside the cylinder valve outlet. It can reduce the maximum flow rate out of a cylinder of PH_3 at 2000 psi from 1.6×10^4 l/min down to 24 l/min, which is low enough to allow other safety systems to adequately process it (20).

Building codes require that compressed toxic gas cylinders be stored in continuously ventilated steel cabinets. We have gone a step further and put all our toxic and flammable gases in a concrete and steel bunker located outside of and adjacent to our processing facility. In addition, remotely actuated emergency shutoff (ESO) valves

are installed in the gas cabinets. They can be actuated from the excess flow switches (EFS) in the purge manifold as well as from the Toxic Gas Detection System (TGDS). The TGDS operates continuously, monitoring the air in the gas cabinet exhaust as well as in various locations near processing equipment in the cleanroom. Seamless, orbitally-welded, electropolished, stainless-steel tubing is used for all process gases to ensure purity. In the case of the toxic gases, all connections are welded except those enclosed in a ventilated cabinet. Exhaust failure alarms are used to close valves in the event that ventilation is lost. In addition, self-contained scrubber units can be used to filter out the small amount of PH_3 purged during a cylinder replacement procedure.

The costs of all these safety features are summarized in Table 2. The calculations are based on a loaded 10-year depreciation of capital expenditures, as well as other features of the IPEG costing strategy (21). We also assumed one cylinder change every 3 months, which would allow even our small 16 liter cylinder of 15% PH_3 in N_2 to supply 4 PDFL diffusion furnace tubes operating at 10 lots/day, 5 days/week for 50 weeks/year. Larger, standard size 44 liter cylinders would reduce unit safety costs even more if larger furnaces are used. The fact that one cylinder can supply many furnaces is the key feature which allows unit capital costs for PH_3-specific safety equipment to be low in a production environment.

TABLE 2
Cost of PH_3-specific capital equipment required to ensure safety.

Item	PDFL cost ($)	Cost/cylinder (4 cylinders)	Cost/furnace (4 furnaces)
FRO	0	0	0
Bunker + Tubing for 4 cylinders	45,000	11,250	2800
Gas Cabinets + purge manifold + ESO valve +EFS	8,100	8,100	2025
TGDS	9,000	2,300	560
Exhaust Alarms	400	100	25
Purge Scrubbers	3,000	3,000	750
Total Capital Cost/Furnace			6160

Using the IPEG formulation, the added capital cost incurred specifically because of using PH_3 is given in Eq. 2.

$$\text{Cost} = \frac{(0.52)\cdot(\text{Capital Cost})}{\text{Annual Production (in MW)}} \qquad (2)$$

Annual production can be calculated using PDFL material usage rate and assuming conservative yield and production rates for industry in Eq. 3.

$$\begin{aligned}\text{Ann. Prod.} &= (100\ \text{cm}^2/\text{wafer})\cdot(50\ \text{wafers/lot})\cdot \\ &\quad (2500\ \text{lots/yr}) \\ &= 1300\ \text{m}^2/\text{yr/furnace} \qquad (3)\end{aligned}$$

This assumes both yield and downtime resulting in the effective usage of 100 cm^2 out of 180 cm^2 available on a 150-mm diameter wafer. Combining Eqs. 2 and 3 gives a PH_3-specific capital cost of:

$$PH_3 \text{ cost} = \frac{(\$6160/\text{furnace})\cdot(0.52/\text{yr})}{1300\ m^2/\text{yr/furnace}}$$
$$= \$2.5/m^2\cdot(0.5\ m^2/\text{lot})$$
$$= \$1.3/\text{lot} \qquad (4)$$

This is only a small fraction of the DOE long-term goal of $\$80/m^2$ for high-efficiency one-sun module costs (22). Assuming a conservative 10% one-sun peak module efficiency results in:

$$PH_3 \text{ cost} = (\$2.5/m^2)/(100W/m^2)$$
$$= \$0.025/W \qquad (5)$$

This would scale approximately inversely with concentration, so that for a 100X concentrator system, the cost would be reduced to 0.02 cents/W, at which point it becomes a negligible part of cell production costs.

A similar cost analysis can be done for capital equipment specifically required for the use of $POCl_3$. The major difference here is that whereas a single cylinder of PH_3 can be piped easily to several furnaces, each furnace must be equipped with its own $POCl_3$ bubbler system if they are to operate simultaneously.

$$POCl_3 \text{ cost} = \frac{(\$8500/\text{furnace})\cdot(0.52/\text{yr})}{(1300\ m^2/\text{yr/furnace})}$$
$$= (\$3.4/m^2)\cdot(0.5\ m^2/\text{lot})$$
$$= \$1.7/\text{lot} \qquad (6)$$

Equation 6 shows that the capital cost incurred when using $POCl_3$ is similar to, if not greater than, that due to the safety systems necessitated by the use of PH_3 in Eq. 4. These capital costs are combined in Table 3 with the material costs calculated earlier in Table 1.

TABLE 3
Material plus capital costs for PH_3 and $POCl_3$.

	PH_3 ($)	$POCl_3$ ($)
Material Cost/Lot	0.10	4.70
Capital Cost/Lot	1.30	1.70
Total Source-Specific Cost/Lot	1.40	6.40

The capital cost projections derived from this analysis have some inherent uncertainty associated with them. However, they do provide a degree of confidence that capital costs are comparable for the two diffusion sources and that they do not overwhelm material utilization costs. Therefore, it can be concluded that PH_3 will be more cost-effective in production environments with output at least as large as that considered here:

Output = (4 cyls)•(4 furns/cyl)•(1300 m^2/yr/furn)
•(100 W/m^2)
= 2 MW/yr for one-sun cells,
= 2 MW/yr•Conc for concentrator cells. (7)

CONCLUSIONS

PH_3 and $POCl_3$ can both produce equivalent low-recombination emitters while maintaining high bulk lifetimes. However, PH_3 may have a higher yield in this regard. In addition, the safety concerns about using PH_3 can be addressed in a cost-effective manner. This gives PH_3 an overall cost advantage over $POCl_3$ when used at multi-megawatt production levels.

ACKNOWLEDGEMENTS

The authors would like to thank P.A. Basore for developing the J_{oe} measurement technique and for the PC-1D simulations, J.M. Gee for characterizing the diffusion furnace, and both of them for many helpful discussions. They are also grateful to M.E. Buck and J.W. Tingley for all the wafer processing that was done.

REFERENCES

PVSC refers to Proceedings of the IEEE Photovoltaics Specialists Conference.

1. R.A. Sinton, Y. Kwark, J.Y. Gan, and R.M. Swanson, Elect. Dev. Lett., 7, p.567, 1986.

2. P. Verlinden, F. Van de Wiele, G. Stehelin, F. Floret, and J.P. Dowd, 19th PVSC, p.405, 1987.

3. R.R. King, R.A. Sinton, R.M. Swanson, and T.F. Ciszek, 19th PVSC, p.1168, 1987.

4. M.A. Green, A.W. Blakers, J. Zhao, A.M. Milne, A. Wang, and X. Dai, IEEE Trans. Elect. Dev., ED-37, (2), p.331, 1990.

5. P.E. Gruenbaum, R.A. Sinton, and R.M. Swanson, Appl. Phys. Lett., 52, p. 1407, 1988.

6. R.R. King, R.A. Sinton, and R.M. Swanson, 20th PVSC, p.538, 1988.

7. R.A. Sinton and R.M. Swanson, 19th PVSC, p.1201, 1987.

8. M.A. Green, Z. Jianhua, A.W. Blakers, M. Taouk, and S. Narayanan, IEEE Elect. Dev. Lett., EDL-7, p.583, 1986.

9. L.A. Christel, SERA Solar Contractor Report, SAND86-7051, Jan. 1987.

10. L.A. Christel, SERA Solar Contractor Report, SAND87-7021, Jan. 1988.

11. Y.H. Kwark and R.M. Swanson, "SIPOS Heterojunction Contacts to Silicon," SAND85-7022, Feb. 1986.

12. D.E. Kane and R.M. Swanson, 18th PVSC, p.578, 1985.

13. R.R. King, R.A. Sinton, and R.M. Swanson, IEEE Trans. Elect. Dev., ED-37, (2), p.365, 1990.

14. P.A. Basore, 21st PVSC, 1990.

15. J.S. Johanessen et al., J. Appl. Phys., 49, p.4453, 1978.

16. S.A. Schwarz et al., J. Vac. Sci. Tech., 15, p.1519, 1978.

17. A. Cuevas, M.A. Balbuena, and R. Galloni, 19th PVSC, p. 918, 1987.

18. A. Morales-Acevedo, J. Appl. Phys., 60, p.815, 1986.

19. P.A. Basore, IEEE Trans. Elect. Dev., ED-37, (2), p.337, 1990.

20. Guardian Gas Protection System, "Flow Rates of Common Semiconductor Gases Through Orifices of Various Sizes," Nov. 13, 1987, GUAR0005:135

21. R.W. Aster and R.G. Chamberlin, JPL Publication 5101-33, Sept. 1977.

22. DOE Five Year Research Plan, 1987-1991, "Photovoltaics: USA Energy Opportunity," 1987, DOE/CH10093-7.

23. J.R. Monkowski, M.D. Monkowski, I.S.T Tsong, and J. Stach, "Hydrogen/Chlorine Distributions in Silicon Dioxide: Detection and Model," Silicon Processing, D.C. Gupta, ed., ASTM Tech. Pub. 804, p. 245, 1983.